Arch. Metall. Mater. **63** (2018), 3, 1379-1383

DOI: 10.24425/123815

K. DYBOWSKI*#, P. KOWALCZYK*, P. KULA*, A. JEZIORNA*, R. ATRASZKIEWICZ*,
Ł. KOŁODZIEJCZYK*, P. ZAWADZKI*, D. NOWAK*, T. KAZIMIERCZAK**, M. KUCIŃSKA***

GRAPHENE-BASED COMPOSITE MEMBRANE FOR WATER DESALINATION

The article presents the results of studies on the efficacy of water desalination (i.e. Elimination of NaCl ions from the solution) using graphene-polyamide composite membranes. The membrane used for filtration consists of a monolayer of polycrystalline graphene on a porous polyamide carrier support (nylon 66). The degree of desalination for an aqueous NaCl solution percolated through the membrane was 18%. In the future this type of membrane may replace the currently used reverse osmosis membranes.

Keywords: graphene, desalination, water filtration, polycrystalline graphene, graphene composite

1. Introduction

Due to its structure and unique properties, graphene may constitute an excellent material for the purification and desalination of water [4,10-12]. Current solutions to achieve these ends are based on reverse osmosis. Osmotic membranes are effective not only in the removal of sodium and chloride ions, but also in the elimination of numerous other impurities present in aqueous media. However, high pressures are required to achieve these goals, which translates into significant energy consumption and limited efficacy of the process. As demonstrated by calculations carried out by a research group at the Massachusetts Institute of Technology (MIT), replacing the osmotic membrane with a layer of graphene may lead to a several-fold increase in the efficacy of the desalting process [1,10,18]. This increase is mainly due to the low thickness of the membrane, being equal to that of a single layer of carbon atoms, combined with its relatively high mechanical strength [1-3,10]. However, as also demonstrated [1,3-4,11,13-17], the graphene layer must feature appropriate defects (pores) so as to provide a barrier against chloride and sodium ions while not retaining water molecules. The induction of defects may reduce the mechanical strength of the graphene layer, thus preventing its application for this particular goal.

The solution proposed in this article is based on polycrystalline graphene monolayers obtained by the method developed at the Institute of Materials Science and Engineering of Lodz University of Technology [5-7]. The method consists in growing graphene films on a liquid metallic phase. The method facilitates the production of continuous, highly ordered and thus strong layers of carbon atoms featuring structural defects such as low-angle grain boundaries, dislocations, and vacancies that can provide efficient filtration [6-9].

2. Material and methods

Graphene for the production of the composite was obtained by the metallurgical method [5]. The substrate for the growth was provided by electrolytic grade copper. The substrate was heated to 1070°C in an argon-hydrogen atmosphere; the pressure within the generator chamber was p_1 = 0.11 MPa. Next, the copper was subjected to low pressure carburizing at T_1 = 1070°C. The chamber was evacuated to the target pressure of p_2 = 10 Pa and the mixture of carbon donor gases and hydrogen was delivered into the chamber in cycles. Carburizing atmosphere was obtained from the decomposition of acetylene and ethylene delivered into the chamber along with hydrogen gas in a 2:2:1 ratio. The carburizing stage consisted of six alternating segments, including the delivery of the carburizing atmosphere over t_b = 5 s and the vacuum annealing for t_d = 600s. After carburization, the growth substrate was heated to T_2 = 1110°C and annealed for t_w = 300s. At this the stage of the process, a layer of graphene is formed on the liquid copper surface. This is due to the change in the solubility of carbon in copper – the solubility of carbon in solid state copper is higher than in the liquid state. After annealing, the substrate was allowed to cool down to the ambient temperature along with the cooling oven.

Metallurgic graphene was analyzed by means of Raman spectroscopy. Renishaw's inVia Raman spectrometer was used for this purpose. The measurements were made using a laser

* INSTITUTE OF MATERIALS SCIENCE AND ENGINEERING, LODZ UNIVERSITY OF TECHNOLOGY, STEFANOWSKIEGO 1/15, 90-924 ŁÓDŹ, POLAND
** R&D DEPARTMENT, AMII SP. Z O.O. [LTD.]
*** NANOMATERIAL STRUCTURAL RESEARCH LABORATORY, BIONANOPARK SP. Z O.O. [LTD.]
# Corresponding author: konrad.dybowski@p.lodz.pl

wavelength of 532 nm; the laser power delivered to the sample was 10 mW. When analyzing the Raman spectra of the graphene, consideration was paid to the presence and the intensity of graphene-specific peaks (G – 1580 cm^{-1} and 2D – (2690 cm^{-1}), as well as of the peaks indicative of the scale of defects within the graphene structure (D – 1350 cm^{-1} and D' – 1620 cm^{-1}). The obtained Raman spectra (Fig. 1) revealed a graphene monolayer being present on the growth substrate. Next, after the growth substrate was etched away and the graphene was transferred onto copper mesh, qualitative examinations of the graphene product were carried out by means of transmission electron microscopy to determine the degree of structural defects at the atomic level. An FEI Talos F200X transmission electron microscope was used for this purpose at atomic resolution and maximum electron-accelerating voltage of V_p = 200 kV.

Following this examination, the obtained polycrystalline graphene layer was transferred via a polymeric carrier (PMMA) from the growth substrate onto the porous polyamide carrier membrane (nylon 66) with an average pore size of 0.1 µm. Commercially available membranes with Ø47 mm were used for this purpose. The graphene that had formed on the metallic substrate was coated with PMMA, and then the metallic substrate was etched away with iron chloride. After the graphene layer was transferred from the growth substrate onto nylon via the PMMA carrier, the PMMA was dissolved in hot acetone vapour. The resulting composite was subjected to further material studies. Surface tests were carried out to assess the continuity of the graphene layer after the transfer. The tests were performed using AFM and SEM microscopes.

Atomic force microscopy was used for the visualization of structural defects at the nanometric scale. Examination was performed using a Bruker Multimode 5 atomic force microscope featuring a Nanoscope V controller. Images were acquired in tapping mode using silicone probes with the spring constant of the beam equal to ca. 40 N/m and at a rated resonance frequency of ca. 300 Hz. Besides the topographic examinations, the measurement involved the recording of the phase contrast, which facilitated the identification of structural incontinuities within the graphene layer.

Micrometric-scale quality or the transfer of the graphene layer onto the nylon carrier was assessed by means of scanning electron spectroscopy. The continuity of graphene layers on insulating supports can be examined by means of the signal of electrons being absorbed by the sample (AEE). The contrast generated during the measurement is due to the differences in currents flowing through the sample depending on whether the electron beam fell within a conductive or a non-conductive area. Dark areas against a light (i.e. Conductive) background indicate the structural incontinuities within the graphene layer on the nylon substrate.

The thus obtained graphene-polyamide membrane was subjected to water filtration tests to examine its efficacy of removal of Na^+ and Cl^- from the aqueous solution. Concentrations of sodium and chloride ions were measured by the conductometric method. Saline solution with a concentration of c_1 = 76 ppm was passed through the membrane; according to the reference curve, the conductivity of the solution was L_o = 172.4 µS/cm. The water stream was delivered at a pressure of p_w = 0.2 MPa. The test solution was prepared from ultrapure deionized water with a conductivity of L = 0. 5 µS/cm. Besides the changes in salt concentrations, changes in the trans-membrane flow were recorded.

3. Results and discussion

As revealed by the Raman spectra of the graphene-polyamide composite, the methodology of the graphene layer transfer used in this study warranted complete coverage of a polyamide substrate with a polycrystalline graphene monolayer. The spectra contained both graphene-specific and nylon-specific peaks (Fig. 2).

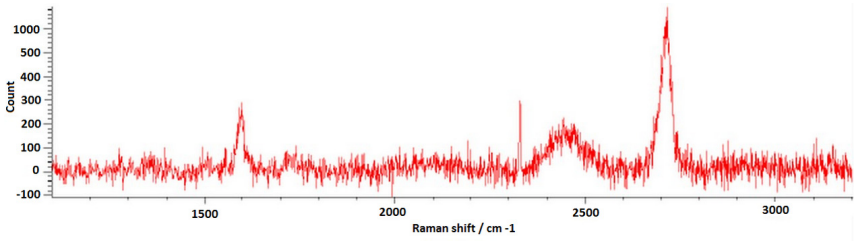

Fig. 1. Raman spectra of graphene on growth substrate

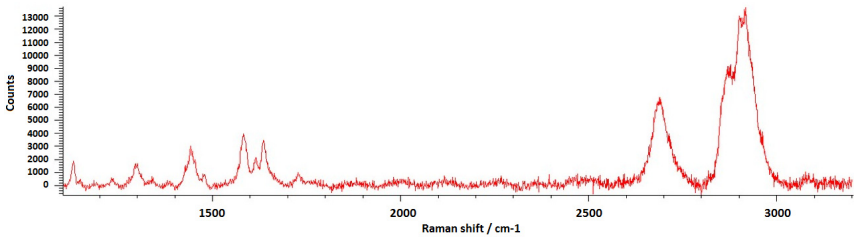

Fig. 2. Raman spectra of a polyamide graphene composite membrane

On the basis of TEM images (Fig. 3), the characteristic honeycomb structure of the monolayer was found to include point vacancy defects sized 2 to 5 Å. In addition, linear defects, i.e. dislocations leading to low-angle grain boundaries, may be observed within the polycrystalline graphene structure (Fig. 4). The maximum measured grain disorientation angle was 7°. The presence of structural defects of the aforementioned type and size is beneficial for the target application. The defects should provide a barrier for sodium and chloride ions while selectively allowing for the passage of water molecules.

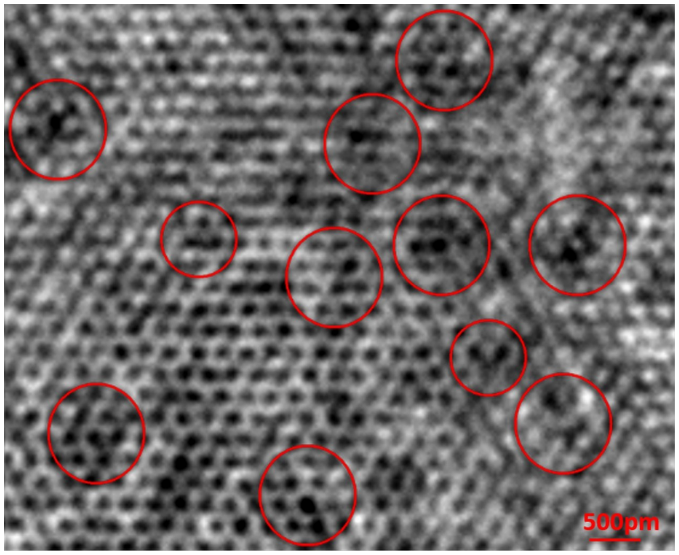

Fig. 3. Point defects of graphene atomic structure obtained by metallurgical method. TEM image

The key factor determining the efficacy of filtration is the presence of defects of a particular size. Too large defects may allow not only water molecules, but also impure ions to pass across the membrane. Therefore, atomic force microscopy was used to characterized the graphene layer defects at the nanometric level. This facilitated the detection of various defects introduced into the structure during the transfer. These include bond breakage, layer breakage, and partial delamination (Fig. 5a,b).

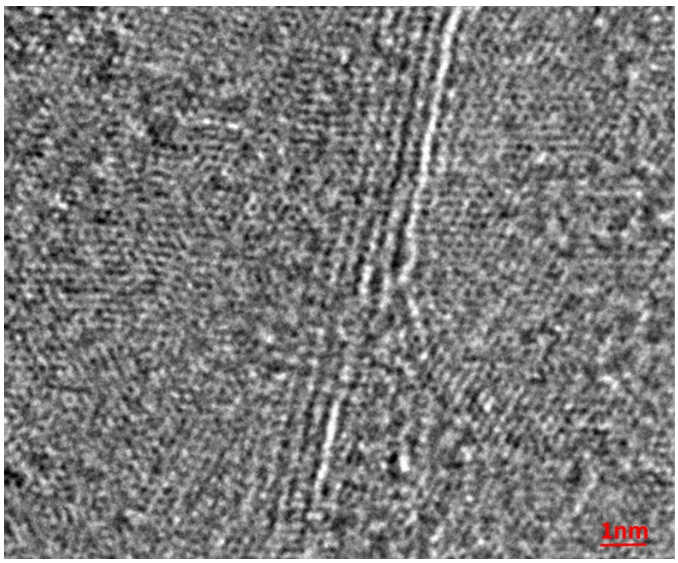

Fig. 4. Linear defects of the graphene atomic structure obtained by the metallurgical method. TEM image

With the transferred areas being this large, the continuity of the graphene layer must also be confirmed at the micro- and macroscopic level; therefore, the surfaces of the membranes were examined after each transfer using an electron scanning microscope with an AEE detector. These examinations unambiguously revealed significant incontinuities, such as layer breakage, delamination, or graphene layer cave-ins within the substrate pores, being present at the micrometric level (Fig. 6a,b). Elimination of these defects by means of improving the transferring technique was required for the desalting effect, and was finally achieved (Fig. 7).

As shown by the results of the water filtration studies, the composite membrane consisting of a monolayer of polycrystalline graphene coated onto a porous carried substrate selectively removed the Na^+ and Cl^- ions from aqueous solutions. The

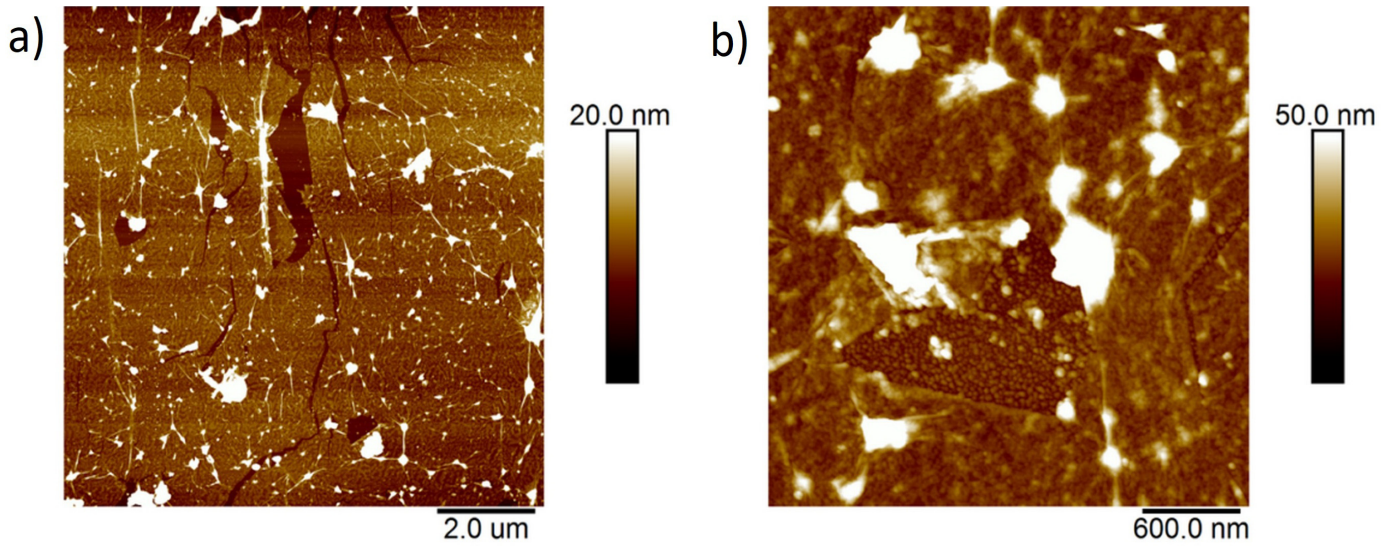

Fig. 5. Defects of the graphene layer resulting from the transfer: a) breakafes, b) partial delamination. AFM image

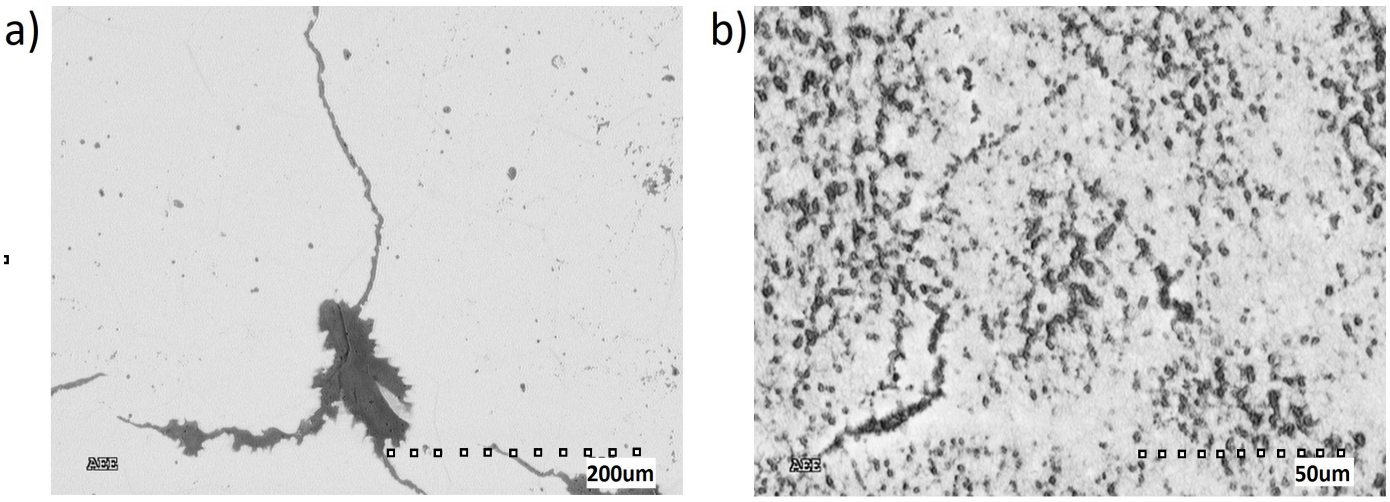

Fig. 6. Defects of the graphene membrane composite layer: a) breakages, partial delamination, b) deposition in the porosity of the substrate. SEM image, AEE detector

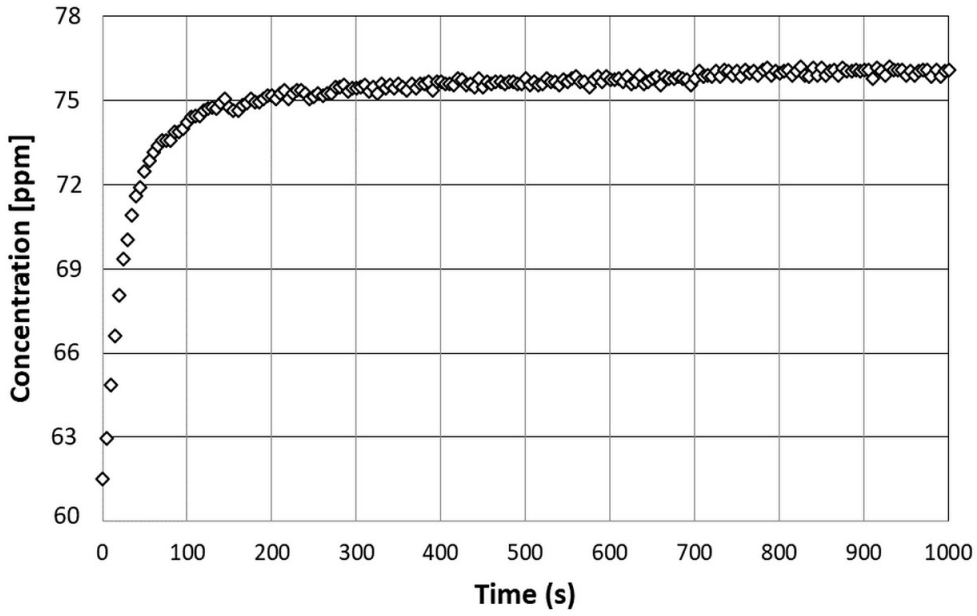

Fig. 7. Changing the concentration of NaCl over time in the water solution as a result of filtration on the composite graphene-polyamide membrane

maximum degree of desalination achieved by the method was about 18%. However, the effect is somewhat short-lived. The highest degree of desalination is observed during the first stage of the process. The desalination defect changes within a period of about 100 seconds starting from a baseline salt level of 62 ppm to reach a level of ca. 74 ppm after 100 seconds. Further on, the effect remains essentially unchanged, reaching ca. 76 ppm after 1000 seconds. This is probably due to the active defects within the graphene structure being blocked as the result of selective retention of chloride and sodium ions, and manifested by the reduced percolation of water (Fig. 8). The flux drops from an initial value of ca. 0.51 l/h/cm^2 to ca. 0.12 l/h/cm^2 after 1000 s and remains constant thereafter, suggesting that the applied pressure does not lead to membrane degradation. The flux of the solution across a nylon membrane devoid of a graphene layer is ca. 0.6 l/h/cm^2.

4. Conclusions

1. The composite membrane consisting of a polycrystalline graphene layer on a polyamide carrier substrate is capable of removing chloride and sodium ions from aqueous NaCl solutions.
2. The low efficiency of the membrane is probably due to the presence of larger defects being generated as the membrane is transferred onto the nylon substrate. Such defects are of several dozen to several hundred nanometers in size, and are difficult to eliminate.
3. The reduced efficacy of desalination observed over time is associated with the drop in the flux of water percolating across the membrane, which indicates that the structural defects are blocked by the impurities being removed.

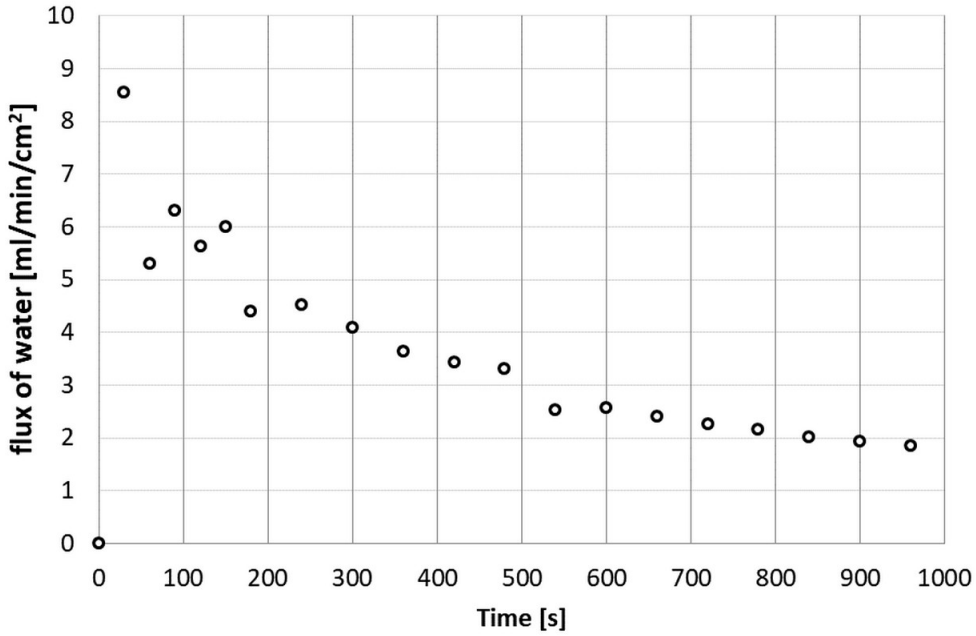

Fig. 8. Changes in flux of water per time during flow through the composite graphene-polyamide membrane

4. An increase in membrane efficiency and elongation of its lifetime would require the elimination of impurities being deposited on the graphene surface during filtration, as well as higher continuity of the graphene layer which constitutes the membrane.

Acknowledgments

The research was funded by the European Union within project no. POIR.04.01.04-00-0089/15, Action 4.1 "Scientific research and development", Sub-measure 4.1.4 "Application projects" Smart Growth Operational Programme 2014 – 2020. Project title: "Graphene based composite for water purification"

REFERENCES

[1] D. Cohen-Tanugi, J. Grossman, Nano Lett. **12** (7), 3602-3608 (2012).
[2] A. Geim, K. Novoselov, Nat. Mater. **6**, 191-283 (2007).
[3] http://www.graphenea. com/pages/graphene-properties (Accessed 25 December 2013).
[4] E. Wang, R. Karnik, Nat. Nanotechnol. 552-554 (2012).
[5] US 9 284 640, USA, Method of producing graphene from liquid metal, P. Kula, A. Rzepkowski. R. Pietrasik, R. Atraszkiewicz, K. Dybowski, W. Modrzyk, (2016).
[6] P. Kula, R. Pietrasik, D. Kazimierski, R. Atraszkiewicz, K. Dybowski, W. Szymański, L. Klimek, P. Niedzielski, M. Cłapa, International journal of nanotechnology **14** (1-6), 191-203 (2017).
[7] Ł. Kołodziejczyk, P. Kula, W. Szymanski, R. Atraszkiewicz, K. Dybowski, R. Pietrasik, Tribology International. **93**, 628-639 Part: B (2014).
[8] P. Kula, W. Szymanski, Ł. Kołodziejczyk, R. Atraszkiewicz, K. Dybowski, J. Grabarczyk, R. Pietrasik, P. Niedzielski, Ł. Kaczmarek, M. Cłapa, Achives of Metallurgy and Materials **60** (4), 2535-2541 (2015).
[9] Z. Gawroński, A. Malasiński, J. Sawicki , Int. J. Automot. Techn. **11** (1), 127-131 (2012).
[10] D. Cohen-Tanugi, R.K. McGovern, S.H. Dave, J.H. Lienhard, J.C. Grossman, Energy Environ. Sci. **7**, 1134-1141 (2014).
[11] D. Konatham, J. Yu, T.A. Ho, A. Striolo, Langmuir **29**, 11884-11897 (2013).
[12] M.E. Suk, N. R. Aluru, J. Phys. Chem. Lett. 1, 1590-1594 (2010).
[13] C. Sun, et al., Langmuir **30**, 675-682 (2014).
[14] S.P. Koenig, L. Wang, J. Pellegrino, J.S. Bunch, Nature Nanotech. **7**, 728-732 (2012).
[15] Y.P. Shan, et al., Nanotechnology **24**, 495102 (2013).
[16] S.P. Surwade, S.N. Smirnov, I.V. Vlassiouk, R.R. Unocic, G.M. Veith, S. Dai, S.M. Mahurin, Nature Nanotechnology **10**, 459-464 (2015).
[17] A. Kumar, M.S. Ramaprabhu, Desalination **282**, 39-45 (2011).
[18] D. Cohen-Tanugi, J.C. Grossman, The Journal of Chemical Physics **141** (7), (2014).